

# **NEGATIVE REFRACTION USING TRUE LEFT-HANDED METAMATERIALS**

A THESIS  
SUBMITTED TO THE DEPARTMENT OF PHYSICS  
AND THE INSTITUTE OF ENGINEERING AND SCIENCE  
OF BİLKENT UNIVERSITY  
IN PARTIAL FULFILLMENT OF THE REQUIREMENTS  
FOR THE DEGREE OF  
MASTER OF SCIENCE

By  
**Koray Aydın**  
September, 2004

I certify that I have read this thesis and that in my opinion it is fully adequate, in scope and in quality, as a dissertation for the degree of Master of Science.

---

Prof. Dr. Ekmel Özbay (Supervisor)

I certify that I have read this thesis and that in my opinion it is fully adequate, in scope and in quality, as a dissertation for the degree of Master of Science.

---

Prof. Dr. Alexander Shumovsky

I certify that I have read this thesis and that in my opinion it is fully adequate, in scope and in quality, as a dissertation for the degree of Master of Science.

---

Assist. Prof. Dr. Vakur B. Ertürk

Approved for the Institute of Engineering and Science:

---

Prof. Dr. Mehmet Baray,  
Director of the Institute of Engineering and Science

# **Abstract**

## **NEGATIVE REFRACTION USING TRUE LEFT-HANDED METAMATERIALS**

**Koray Aydın**

M. S. in Physics

Supervisor: Prof. Dr. Ekmel Özbay

September 2004

Left-handed materials and negative refraction attracted a great amount of attention in recent years due to their unique physical properties. It is possible to obtain a left-handed material by combining a novel artificial structure (split ring resonator) and a wire structure periodically. We investigated the transmission and reflection properties of split ring resonators (SRR), wires and composite metamaterials consisting of SRR and wire structures. We have successfully demonstrated true left-handed behavior in free space with a high transmission peak (-1.2 dB). This is the highest transmission peak reported for a left-handed material. The left-handed transmission band coincides exactly with the region where both dielectric permittivity and magnetic permeability have negative values. We proposed and demonstrated a new method to distinguish the magnetic resonance of the SRR structures.

We experimentally confirmed that composite metamaterial has a negative refractive index, at the frequencies where left-handed transmission takes place. Phase shift between consecutive numbers of layers of CMM is measured and phase velocity is shown to be negative at the relevant frequency range. Refractive index values obtained from the refraction experiments (-1.87) and the phase shift experiments (-1.78) are in good agreement.

**Keywords:** Left-Handed Material, Composite Metamaterial, Split Ring Resonator, Negative Permittivity, Negative Permeability, Effective Medium Theory, Photonic Band Gap, Negative Refraction, Negative Phase Velocity.

# Özet

## GERÇEK SOLAK MATERYALLER KULLANILARAK NEGATİF KIRILMA ELDE EDİLMESİ

**Koray Aydın**

Fizik Yüksek Lisans

Tez Yöneticisi: Prof. Dr. Ekmel Özbay

Eylül 2004

Solak materyaller ve negatif kırılma kendilerine has fiziksel özellikleri dolayısıyla günümüzde oldukça ilgi çeken konular haline gelmişlerdir. Yeni bir yapay yapı olan yarıkli halka rezonatörleri ve ince tel yapıları kullanılarak solak materyal elde etmek mümkündür. Bu çalışmada yarıkli halka rezonatörleri, tel yapıları ve bu ikisinin bir araya getirilmesiyle oluşan karma ara-maddelerde geçirgenlik ve yansıma özelliklerini inceledik. Gerçek solak davranış sergileyen ve yüksek geçirgenliğe (-1.2 dB) sahip olan karma ara-maddeler başarıyla gösterildi. Bu geçirgenlik değeri bugüne kadar rapor edilmiş olan en yüksek değerdir. Solak geçirgenlik bandı hem dielektrik permitivite hem de magnetik permeabilitenin eksi değerler aldığı frekans bölgesinde yer almaktadır. Yarıkli halka rezonatörlerinin magnetik rezonansını belirleyebilmek için yeni bir metod geliştirdik ve bu metodu deneysel olarak da doğruladık.

Solak geirgenliđin olduđu frekans aralıđında karma ara-maddenin eksi kırılma indeksine sahip olduđunu deneysel olarak kanıtladık. İki farklı uzunluktaki karma ara-maddelerin faz farkı ölçölmek suretiyle, ilgili frekans aralıklarında bu yapıların eksi faz hızına sahip oldukları gösterildi. Kırılma deneyinden elde edilen kırılma indeksi (-1.87) ile faz farkından hesaplanan kırılma indeksi (-1.78) birbirlerine oldukça yakın deđerlere sahiptirler.

**Anahtar Sözcükler:** Solak Materyal, Karma Ara-Madde, Yarıklı Halka Rezonatörü, Negatif Permittivite, Negatif Permeabilite, Efektif Ortam Teorisi, Fotonik Bant Aralığı, Negatif Kırılma, Negatif Faz Hızı.

# Acknowledgements

It is my pleasure to express my deepest gratitude and respect to Prof. Dr. Ekmel Özbay for his invaluable guidance, helpful suggestions and endless support. His personal and academic virtue shaped my academic personality and changed my approach to scientific study. I am very lucky to have the opportunity to study under his tutelage.

I would like to thank to the members of my thesis committee, Prof. Dr. Alexander Shumovsky and Assist. Prof. Dr. Vakur B. Ertürk, for reading the manuscript and commenting on the thesis.

Very special thanks to Dr. Mehmet Bayındır from whom I learnt a lot, including the importance of hard work. His invaluable advice and superior motivation during my difficult times kept me standing. I am also indebted to Ertuğrul Çubukçu for his help, understanding and friendship. I appreciate Dr. Kaan Güven for his great advice, endless help and continuous support during my research.

I would like to thank my office mates, Necmi Bıyıklı, İbrahim Kimukin, İrfan Bulu, Süheyla Sena Akarca Bıyıklı, Bayram Bütün, Hümeyra Çağlayan and Turgut Tut for creating a fruitful working environment. It is a great pleasure to work together with such nice and hardworking friends.

I am also thankful to my friends in the physics department, Muhammed Yönaç, Yavuz Öztürk, Rasim Volga Ovali, Serdar Özdemir, Levent Subaşı, Engin Durgun, Sefa Dağ, Aşkın Kocabaş, and Sinem Binicioğlu Çetiner. Your friendship is invaluable to me. And Emine “Abla”, thank you as well, for making my life easier.

There is a long list of my close friends, whether old or new, far away of nearby; to feel their existence is my life source. Thank you all.

I would like to express my endless thanks to my mother, father and sister for their love, encouragement and care. I would also thank to my new family, who doubled the support and encouragement I have.

Finally, special thanks go to my wife, **Elif**, for her boundless love, endless trust and for shining a different color onto my life. I cannot imagine finishing all my achievements without her endless moral support. I dedicate this labor to her.



# Contents

<b>Abstract</b>	<b>i</b>
<b>Özet</b>	<b>iii</b>
<b>Acknowledgements</b>	<b>v</b>
<b>Contents</b>	<b>vii</b>
<b>List of Figures</b>	<b>x</b>
<b>1 Introduction</b>	<b>1</b>
<b>2 Theoretical Background</b>	<b>6</b>
2.1 Introduction .....	6
2.2 Negative Permittivity ( $\epsilon < 0$ ) .....	9
2.3 Negative Permeability ( $\mu < 0$ ) .....	13
2.4 Negative Refraction .....	19
<b>3 10 GHz Composite Metamaterials</b>	<b>25</b>
3.1 Introduction .....	25
3.2 Transmission and Reflection Experiments .....	26
3.2.1 Experimental Setup .....	26
3.2.2 Structures .....	29
3.3 Transmission and Reflection Characteristics .....	30
3.3.1 Periodic “Discontinuous Thin Wire” Medium .....	30
3.3.2 Periodic “Split Ring Resonator” Medium .....	33
3.3.3 Composite Metamaterial .....	36

3.4 Summary .....	38
<b>4 True Left-Handed Metamaterial</b>	<b>40</b>
4.1 Introduction .....	40
4.2 Magnetic Resonance Gap of SRR Structure .....	41
4.2.1 Band gap formation analysis for SRR Periodic Structure.	41
4.2.2 Effect of Misalignment and Periodicity on the Magnetic Resonance Gap .....	45
4.3 Electric Responses .....	48
4.3.1 Comparison of Continuous and Discontinuous Wire Structures .....	48
4.3.2 Downward plasma frequency shift for CMM Structures due to SRR's electric response .....	50
4.4 True Left-Handed Transmission Peak .....	52
4.5 Summary .....	54
<b>5 Negative Refraction of 2D LHMs</b>	<b>55</b>
5.1 Introduction .....	55
5.2 Transmission Through 2D LHM .....	56
5.3 Negative Refraction in 2D LHMs .....	60
5.3.1 Negative Refraction Experimental Setup .....	60
5.3.2 Experimental Verification of Negative Refraction .....	63
5.4 Negative Phase Velocity .....	66
5.4.1 Experimental Verification of Negative Phase Velocity ...	66
5.4.2 Index of Refraction Calculation from Phase Shift .....	68
5.5 Summary .....	71

<b>6 Conclusions and Future Directions</b>	<b>72</b>
<b>List of Publications</b>	<b>74</b>
<b>Bibliography</b>	<b>76</b>

# List of Figures

1.1	Examples of Negative refractive media (a) Left-handed metamaterials, (b) 2D Photonic Crystals.	3
2.1	$\epsilon$ and $\mu$ space. 3 <sup>rd</sup> region shows left-handed medium.	8
2.2	A periodic configuration of thin metallic wires with a lattice spacing of $a$ and radius $r$ .	11
2.3	Schematic drawings of (a) Single split ring resonator(SRR) (b) SRRs grouped into a periodic array	14
2.4	Resonance for effective permeability of SRRs	16
2.5	Magnetic field polarized (a) along the split ring axis, (b) perpendicular to the split ring axis	18
2.6	Schematic drawing of incident (1), reflected (2), negatively refracted (3) and positively refracted (4) beams	20
2.7	Beam path in (a) rectangular, (b) convex, (c) concave lenses made of left-handed materials	23
3.1	Experimental setup for transmission measurements	27
3.2	Horn antennas used to scan frequency regions (a) 3-7 GHz, (b) 7-14 GHz, (c) 10-22 GHz	27
3.3	Experimental setup for reflection measurements	28
3.4	Pictures of PCB boards consisting of (a) 15x15 SRR array, (b) 15x15 discontinuous wire array	30
3.5	Schematic drawings of (a) two wire strips separated by a gap, (b) periodical arrangement of discontinuous wire strips	31

3.6	Measured transmission and reflection spectra of the discontinuous thin wire medium .....	32
3.7	Schematics of (a) single SRR unit, (b) periodical arrangement of SRRs	34
3.8	Measured transmission and reflection spectra of the periodic split ring resonator medium .....	35
3.9	Measured delay time, photon lifetime, as a function of frequency. The delay time increases rapidly as we approach the band edges .....	36
3.10	Schematic drawing of periodically arranged composite metamaterial composed of alternating layers of SRRs and wires .....	37
3.11	Measured transmission and reflection spectra of the composite metamaterial . .....	38
4.1	Schematics of (a) a single split ring resonator (SRR) (b) a ring resonator with splits closed (CSRR) (c) Periodic CMM composed of SRRs on one side, wires on the other side of dielectric board . .....	42
4.2	Measured transmission spectra of a periodic SRR medium (solid line) and periodic CSRR medium (dashed line) between (a) 3-14 GHz, (b) 3-7 GHz .....	44
4.3	(a) Measured transmission spectra of aligned (solid line) and slightly misaligned (dashed line) SRR structures. (b) Top view of aligned SRRs. (c) Top view of slightly misaligned SRRs .....	46
4.4	(a) Measured transmission spectra of aligned and hardly misaligned SRR structures. (b) Top view of hardly misaligned SRRs .....	47
4.5	(a) Measured transmission spectra of periodic (solid line) and non-periodic (dashed line) SRR structures. (b) Front view of non-periodic	

	SRRs .....	47
4.6	Measured transmission spectra of continuous (solid line) and discontinuous wires (dashed line) .....	49
4.7	Measured transmission spectra of wires (dashed line) and closed CMM (solid line) composed by arranging closed SRRs and wires periodically	51
4.8	Transmission spectra of SRRs (solid line), wires (dashed line) and composite metamaterial (bold solid line) .....	53
5.1	Schematic drawing of 2D CMM structure. Shaded area shows the unit cell of the structure .....	58
5.2	Measured transmission spectra of a periodic SRR medium (solid line) and periodic CSRR medium (dashed line) between (a) 3-14 GHz, (b) 3-7 GHz .....	59
5.3	Schematic drawing of refraction of incident beam passing from a wedge sample to air. Both positive and negative refraction cases are sketched .....	61
5.4	Schematic drawing of experimental setup used for negative refraction experiment .....	62
5.5	2D wedge structure .....	63
5.6	Measured intensity spectrum of wedge shaped LHM sample as a function of frequency and refraction angle .....	64
5.7	The angular cross section of transmitted beam at 3.92 GHz .....	65
5.8	Unwrapped transmission phase data obtained from different lengths of CMM between 5.4 - 7.0 GHz, where right-handed transmission peak takes place. Inset: Average phase difference between consecutive	

	numbers of layers of CMM. Phase shift is positive between 5.4 - 7.0 GHz.....	67
5.9	Unwrapped transmission phase data obtained from different lengths of CMM between 3.73 - 4.05 GHz, where left-handed transmission peak takes place. Inset: Average phase difference between consecutive numbers of layers of CMM. Phase shift is negative between 3.73 - 4.05 GHz .....	68
5.10	The values of negative refractive indices obtained by using two experimental methods; the refraction experiments and the phase shift measurements. There is a quite good agreement for the values of negative refractive indices for these two experimental methods .....	70

*I do not know what I may appear to the world, but to myself I seem to have been only a boy playing on the sea-shore, and diverting myself in now and then finding a smoother pebble or a prettier shell than ordinary, whilst the great ocean of truth lay all undiscovered before me.*

*Isaac Newton*



# Chapter 1

## Introduction

Left-handed materials and negative refraction phenomena have been studied extensively in recent years due to their unique physical properties and novel applications. Negative refraction of electromagnetic waves is the most interesting physical phenomena behind the left-handed metamaterial structures. The reversal of Doppler shift and backward Cerenkov radiation are also unusual physical characteristics arising from left-handed materials.

The electric and magnetic properties of materials are determined by two important material parameters, dielectric permittivity and magnetic permeability. Together the permeability and the permittivity determine the response of the material to the electromagnetic radiation. Generally,  $\epsilon$  and  $\mu$  are both positive in ordinary materials. While  $\epsilon$  could be negative in some materials (for instance,  $\epsilon$  possesses negative values below the plasma frequency of metals), no natural materials with negative  $\mu$  are known. However, for certain structures, which are called left-handed materials (LHM), both the effective permittivity,  $\epsilon_{eff}$  and permeability,  $\mu_{eff}$  possess negative values. In such materials the index of refraction,  $n$ , is less than zero, and therefore, phase and group velocity of an electromagnetic (EM) wave can propagate in opposite directions such that the direction of propagation is reversed with respect to the

direction of energy flow [1]. This phenomenon is called the negative index of refraction and was first theoretically proposed by Veselago in 1968, who also investigated various interesting optical properties of the negative index structures [1].

Negative effective permittivity in the microwave frequency range can be achieved by using periodic thin wire media. Dielectric permittivity takes negative values and EM waves cannot propagate inside the medium below the plasma frequency [2-4]. Electric charge is responsible for a large electric response in dielectric materials. Because of the lack of magnetic charge analogous to electric charge, it is more difficult to obtain a material with negative magnetic permeability. Pendry *et al.* suggested that a periodic array of artificial structures called split ring resonators (SRRs) exhibit negative effective  $\mu$  for frequencies close to the magnetic resonance frequency [5]. Smith *et al.* reported the experimental demonstration of left-handed materials by stacking SRR and thin wire structures as arrays of 1D and 2D structured composite metamaterials (CMM). [6,7].

Theoretical calculations and analyses showed that the refractive index is indeed negative, where both  $\epsilon$  and  $\mu$  are simultaneously negative [1,8]. Experimental observation of negative refraction in left-handed materials is verified by Shelby *et al.* [9]. Negative refraction, and in general, wave propagation in negative index media have also been a controversial subject and have generated an intense debate. Valanju *et al.* claimed that dispersion implies positive refraction of group velocity even when the phase velocity is refracted negatively [10]. Effects of dispersion and loss on negative refraction experiments [11], and perfect lens behavior of left-handed materials [12] are

criticized. But further experimental studies on negative refraction, addressing the issues criticized, using different techniques supported the existence of negative refraction [13,14].

On the other hand, composite metamaterials (Fig 1.1(a)) are not the only materials that give rise to the negative refraction concept. Negative refraction is also achievable by using 2D photonic crystals (PCs) (Fig 1.1(b)). Theoretical studies [15-17] and experimental observations [18-20] confirmed the existence of the negative refractive index for 2D PCs. Negative refraction using 2D PCs has a different physical origin and the argument on negative values of  $\epsilon$  and  $\mu$  is not used. The equal frequency contours of PC and air, and the conservation of the parallel wave-vector component form the basis of the negative refraction idea in 2D photonic crystals [21].

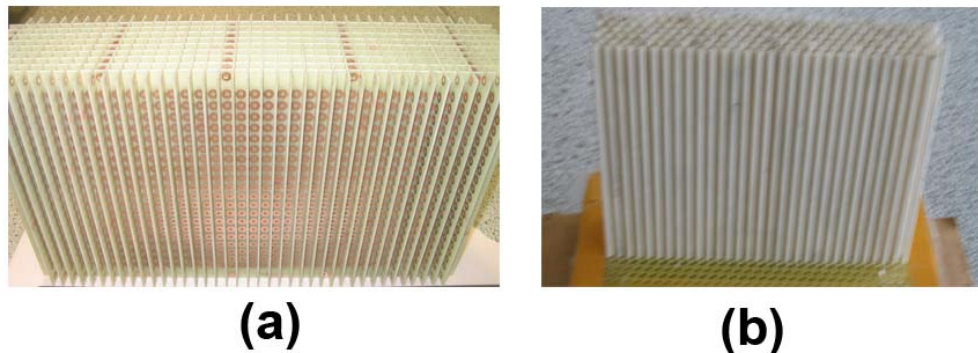


Fig 1.1: Examples of Negative refractive media (a) Left-handed metamaterials, (b) 2D Photonic Crystals.

Left-handed materials can be used in several applications. A perfect lens is a possible application. An unconventional alternative to a lens, a slab of negative refractive index material, has the power to focus all Fourier components of a

2D image, even those that do not propagate in a radiative manner [22]. Reversals of Doppler effect [23] and Cerenkov radiation[24], backward wave propagation[25], are the other interesting physical phenomena rising from the negative refractive concept. Moreover, structures with negative  $\mu$ , can be used for magnetic resonance imaging [26].

This thesis will be organized as follows. In the second chapter, we will have a theoretical introduction to left-handed materials and its components. We will discuss how to achieve negative permittivity and negative permeability at the microwave frequency range. Later we will show how to obtain a negative refractive index medium, using negative permittivity and negative permeability media together. In the third chapter, the transmission characteristics of SRRs, wires and CMMs in free space will be considered. Most of the work presented in chapter 3 appeared as a journal article in IEEE Transactions on Antennas and Propagation [27].

In chapter 4, we first identify the magnetic resonance and electric resonance of SRRs by using ring resonators with the splits closed. We then verify the effect of the interaction between SRRs and wires and demonstrate experimentally the shift in plasma frequency. Finally we present a new CMM structure that exhibits true left-handed behavior and has a transmission band with a peak value at -1.2 dB. Some of the achievements represented in chapter 4 are to appear as a journal article in Optics Letters [28]. In chapter 5, we demonstrate a negative refractive index in left-handed metamaterials. Then we present direct experimental evidence that the phase velocity is negative within the left-handed pass band of a CMM. Some of the contents of chapter 5 have been submitted to Applied Physics Letters [29]. The last chapter will include a

brief summary of the results obtained during this thesis work. Future perspectives and directions will also be provided in this chapter.

# Chapter 2

## Theoretical Background

### 2.1 Introduction

The dielectric constant  $\epsilon$  and the magnetic permeability  $\mu$  are the fundamental characteristic quantities that determine the propagation of electromagnetic waves in matter. This is due to the fact that they are the only material parameters appearing in the dispersion equation

$$\left| \frac{\omega^2}{c^2} \epsilon_{ij} \mu_{ij} - k^2 \delta_{ij} + k_i k_j \right| = 0 \quad (2.1)$$

which gives the relation between the frequency  $\omega$  of a monochromatic wave and its wave vector  $k$ . For an isotropic substance Eq. (2.1) takes a simpler form:

$$k^2 = \frac{\omega^2}{c^2} n^2 \quad (2.2)$$

where  $n^2$  is given by

$$n^2 = \epsilon \mu \quad (2.3)$$

From Eqs. (2.2) and (2.3), one can say that a simultaneous change of the signs of  $\epsilon$  and  $\mu$  has no effect on these relations [1]. But as we will see in the upcoming parts of this chapter, materials having simultaneously negative

values of  $\varepsilon$  and  $\mu$  have some physical properties and unique characteristics that are different from those of ordinary materials having positive  $\varepsilon$  and  $\mu$ .

To understand the effect of changes in the signs of  $\varepsilon$  and  $\mu$ , we have to consider the initial Maxwell equations, where  $\varepsilon$  and  $\mu$  appear separately, different from equations Eqs. (2.1), (2.2) and (2.3) where their product appears in the equations [1]. Primarily Maxwell equations

$$\begin{aligned}\nabla \times \mathbf{E} &= -\frac{1}{c} \frac{\partial \mathbf{B}}{\partial t} \\ \nabla \times \mathbf{H} &= \frac{1}{c} \frac{\partial \mathbf{D}}{\partial t}\end{aligned}\tag{2.4}$$

and constitutive relations

$$\begin{aligned}\mathbf{B} &= \mu \mathbf{H} \\ \mathbf{D} &= \varepsilon \mathbf{E}\end{aligned}\tag{2.5}$$

are given. For a monochromatic plane wave, all quantities are proportional to  $e^{i(kz-\omega t)}$  and therefore Eqs. (2.4) and (2.5) reduce to

$$\begin{aligned}\mathbf{k} \times \mathbf{E} &= \frac{\omega}{c} \mu \mathbf{H} \\ \mathbf{k} \times \mathbf{H} &= -\frac{\omega}{c} \varepsilon \mathbf{E}\end{aligned}\tag{2.6}$$

These are the key expressions to understand the problem of left-handed materials. If both  $\varepsilon$  and  $\mu$  are positive, it is clearly seen that  $\mathbf{E}$ ,  $\mathbf{H}$  and  $\mathbf{k}$  form a right-handed triplet of vectors. The interesting point is that for simultaneously negative values of  $\varepsilon$  and  $\mu$ , a left-handed vector triplet of  $\mathbf{E}$ ,  $\mathbf{H}$  and  $\mathbf{k}$  is formed. At the same time, the direction of the energy flow determined by the Poynting vector  $\mathbf{S}$  is independent of the signs and values of  $\varepsilon$  and  $\mu$ :

$$\mathbf{S} = \frac{c}{4\pi} \mathbf{E} \times \mathbf{B} \quad (2.7)$$

Poynting vector is always directed away from the source of the radiation. But amazingly the  $\mathbf{k}$  vector may be directed away from the source (for the cases where  $\epsilon$  and  $\mu$  are both positive) or towards the source (for the cases where  $\epsilon$  and  $\mu$  are both negative). This is the major difference between the case with negative  $\epsilon$  and  $\mu$  values and the case with corresponding positive values [1].

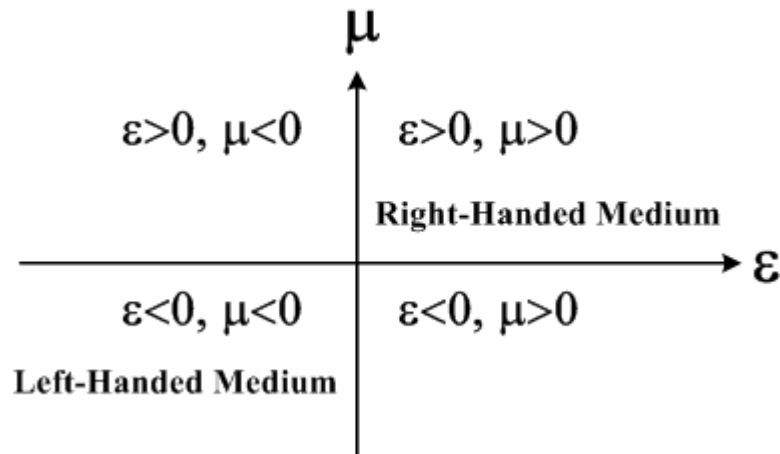


Figure 2.1:  $\epsilon$  and  $\mu$  space. 3<sup>rd</sup> region shows left-handed medium.

Figure 2.1 shows  $\epsilon$  and  $\mu$  space. Ordinary materials having  $\epsilon > 0$  and  $\mu > 0$  allow the propagation of EM waves, and they have positive refractive index values hence they can be called right-handed media. Since one of the permittivity or permeability values is negative and the other is positive at the second and fourth parts of  $\epsilon$  and  $\mu$  space, EM waves cannot propagate inside the medium and evanescent waves will occur. For the third part of the  $\epsilon$  and  $\mu$  space, since the product of  $\epsilon$  and  $\mu$  are positive, EM waves can propagate inside



the medium. This part is the left-handed media part, since both  $\varepsilon$  and  $\mu$  are simultaneously negative as will be discussed later in this chapter.

## 2.2 Negative Permittivity ( $\varepsilon < 0$ )

Plasma is a medium with an equal concentration of positive and negative charges, of which at least one charge type is mobile. In a solid, the negative charges of the conduction electrons are balanced by an equal concentration of positive charge of the ion cores [30].

The polarization of a collection of atoms or molecules can rise in two ways: a) The applied field distorts the charge distributions and so it produces an induced dipole moment in each molecule; b) the applied field tends to line up the initially randomly oriented permanent dipole moments of the molecules. To estimate the induced moments we consider a simple model of harmonically bound charges (electrons and ions) [31]. Each charge  $e$  is bound under the action of a restoring force

$$\mathbf{F} = -m\omega_0^2 \mathbf{x} \quad (2.8)$$

where  $m$  is the mass of the charge, and  $\omega_0$  is the frequency of oscillation about equilibrium. The equation of motion for an electron of charge  $-e$  bound by a harmonic force (Eq. 2.8) and acted by an electric field  $\mathbf{E}(\mathbf{x}, t)$  is given by

$$m[\ddot{\mathbf{x}} + \gamma\dot{\mathbf{x}} + \omega_0^2 \mathbf{x}] = -e\mathbf{E}(\mathbf{x}, t) \quad (2.9)$$

where  $\gamma$  is a damping term representing dissipation of the plasmon's energy into the system. An approximation can be made taking into account that the amplitude of the oscillation is small enough to permit the evaluation of the

electric field at the average position of the electron. If the field varies harmonically in time with the frequency  $\omega$  as  $e^{-i\omega t}$ , the dipole moment contributed by one electron is

$$\mathbf{p} = -e\mathbf{x} = \frac{e^2}{m}(\omega_0^2 - \omega^2 - i\omega\gamma)^{-1}\mathbf{E} \quad (2.10)$$

If we suppose that there are  $N$  molecules per unit volume with  $Z$  electrons per molecule, and that, instead of a single binding frequency for all, there are  $f_j$  electrons per molecule with a binding frequency  $\omega_j$  and damping constant  $\gamma_j$ , then the dielectric constant is given by [31]

$$\frac{\varepsilon(\omega)}{\varepsilon_0} = 1 + \frac{Ne^2}{\varepsilon_0 m} \sum_j f_j (\omega_j^2 - \omega^2 - i\omega\gamma_j)^{-1} \quad (2.11)$$

At frequencies far above the highest resonant frequency the dielectric constant takes on the simplest form

$$\varepsilon(\omega) = 1 - \frac{\omega_p^2}{\omega(\omega + i\gamma)} \quad (2.12)$$

which is approximately independent of the wave vector,  $\mathbf{k}$ . The significant point about Eq. (2.12) is that,  $\varepsilon(\omega)$  is essentially negative below the plasma frequency ( $\omega_p$ ), at least down to frequencies comparable to  $\gamma$ . A longitudinal mode, the plasmon, appears at a fixed frequency, and two longitudinal modes emerge at the plasma frequency. In consequence of the negative  $\varepsilon$ , only evanescent modes (imaginary wave vector) exist below the plasma frequency and below this threshold no radiation penetrates very far into the metal [2].

The frequency  $\omega_p$ , which depends only on the total number of  $n = NZ$  of electrons per unit volume is given by the formula

$$\omega_p^2 = \frac{ne^2}{\epsilon_0 m_{eff}} \quad (2.13)$$

In simple metals  $\gamma$  is small relative to  $\omega_p$ . For instance  $\omega_p = 15$  eV whereas  $\gamma = 0.1$  eV for aluminum [2].

The electromagnetic response is dominated by negative permittivity concept in the visible and UV frequency regions. However, at lower frequencies starting from the near infrared and downwards, dissipation asserts itself, therefore dielectric function becomes imaginary. To achieve negative permittivity values at microwave range, the thin metallic wire concept is proposed [2,3]. Also loop-wire medium is investigated for the same purposes [4].

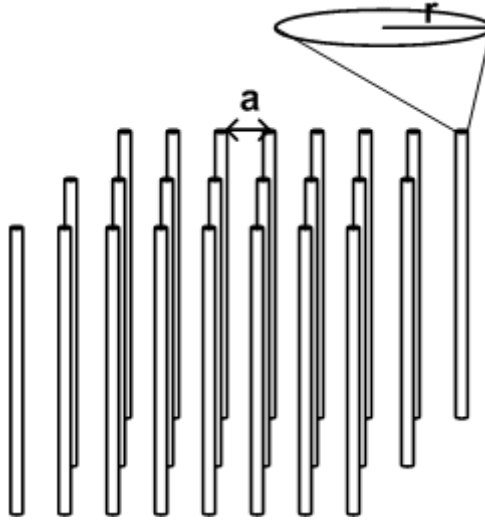


Figure 2.2: A periodic configuration of thin metallic wires with a lattice spacing of  $a$  and radius  $r$ .

By assembling thin metallic wire structures into a periodic medium (Fig 2.2) with appropriate parameters, negative permittivity can easily be achieved at microwave frequencies. Plasma frequency of the thin metallic wires is given after detailed calculations as [2]

$$\omega_p^2 = \frac{ne^2}{\epsilon_0 m_{eff}} = \frac{2\pi c_0^2}{a^2 \ln(a/r)} \quad (2.14)$$

where  $c_0$  is the speed of light in free space,  $a$  is the lattice parameter and  $r$  is the radius of the wires.

Note that although the newly reduced plasma frequency can be expressed in terms of electron effective mass and charge, these microscopic quantities cancel, leaving a formula containing only macroscopic parameters of the system: radius of the wires, and periodicity of the wire medium.

The metallic wires were structured on a scale much less than the wavelength of radiation. When the wavelength of the incident radiation is much larger than the size and spacing of a collection of scatterers, the response of the scatterers to the incident fields can be treated by way of the effective medium theory.

$$a \ll \lambda = 2\pi c_0 \omega^{-1} \quad (2.15)$$

In the thin wire case, the effective medium theory holds since corresponding  $\lambda$  for  $\omega_p$  is much larger than the radius of the wires. Therefore, an effective dielectric permittivity,  $\epsilon_{eff}$  can be used to define the permittivity of the medium. As far as external electromagnetic radiation is concerned, a thin wire structure appears as an effectively homogeneous dielectric medium whose internal structure is only apparent as it dictates  $\epsilon_{eff}$ . In this respect it is important that the

structure be made of thin wires. Eq. (2.14) shows that the function of the small radius is to suppress the plasma frequency. For a thick wire structure in Eq. (2.14),  $\ln(a/r) \approx 1$  so that the plasma frequency corresponds to a free space wavelength of approximately twice the lattice spacing. Therefore, Bragg diffraction effects would interfere with our simple plasmon picture. Choosing a small radius ensures that diffraction occurs only at much higher frequencies.

## 2.2 Negative Permeability ( $\mu < 0$ )

Electric charge is responsible for large electric response in dielectric materials. Because of the lack of magnetic charge analogous to an electric charge, it is more difficult to obtain a material with negative magnetic permeability. Naturally occurring materials almost universally have a positive permeability, and thus a left-handed material, while not ruled out by fundamental considerations, seemed unlikely to be practical. However, in 1999, Pendry *et al.* [5] introduced several configurations of conducting scattering elements displaying a magnetic response to an applied electromagnetic field when grouped into an interacting periodic array.

Usually the magnetic permeability equals to unity ( $\mu = 1$ ) for ordinary materials. Thin metallic wire media discussed in the previous section of this chapter responds to the electric field and dielectric permittivity becomes negative below the plasma frequency of the wires. But these metallic wire structures do not give any response to the magnetic field. So in order to obtain negative permeability, one has to extend the magnetic properties of the materials. Pendry *et al.* [5], enhanced the magnetic response of artificially designed materials by introducing capacitive elements into the structure.

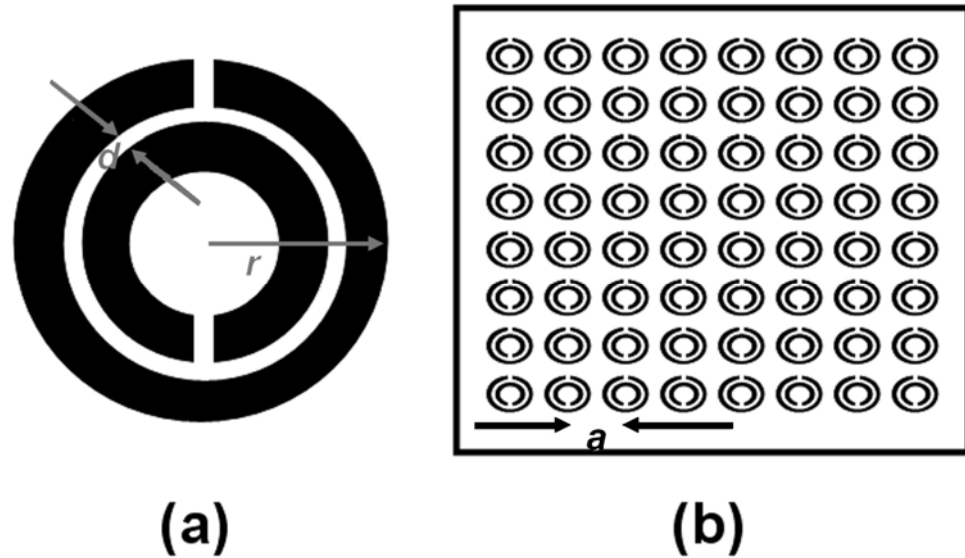


Figure 2.3: Schematic drawings of (a) Single split ring resonator (SRR) (b) SRRs grouped into a periodic array.

Figure 2.3(a) shows the design of Pendry, described as a split ring resonator (SRR) [5]. In a split ring resonator there are two rings both having a split. By having splits in the rings, the SRR unit can be made resonant at wavelengths much larger than the diameter of the rings. The purpose of the second split ring, inside and whose split is oriented oppositely to the outside split, is to generate a large capacitance in the small gap region. The gap between the rings prevents current from flowing around any one ring. However, there is a considerable capacitance between the two rings, which enables current to flow. By combining the SRRs into a periodic medium, (Fig. 2.3(b)) such that there is strong magnetic coupling between the resonators, unique properties emerge from the composite and isotropy can be achieved.

Structures having effective permeability and permittivity comply with the following equation

$$\begin{aligned}\mathbf{B}_{\text{ave}} &= \mu_{\text{eff}} \mu_0 \mathbf{H}_{\text{ave}} \\ \mathbf{D}_{\text{ave}} &= \varepsilon_{\text{eff}} \varepsilon_0 \mathbf{E}_{\text{ave}}\end{aligned}\quad (2.16)$$

where we assume that the structure is on a scale much shorter than the wavelength of any radiation, in order to enable the ability for us to talk about an average value for all of the fields.

Detailed calculations [5] give effective permeability of the SRR to be

$$\mu_{\text{eff}} = 1 - \frac{F}{1 + \frac{2\sigma i}{\omega r \mu_0} - \frac{3}{\pi^2 \mu_0 \omega^2 C r^3}} \quad (2.17)$$

where  $F$  is the fractional volume of the cell, and  $r$  is the radius of the outer ring

$$F = \frac{\pi r^2}{a^2} \quad (2.18)$$

$C$  is the capacitance per unit area, and  $a$  is the lattice constant,

$$C = \frac{\varepsilon_0}{d} = \frac{1}{d c_0^2 \mu_0} \quad (2.19)$$

where  $d$  is the distance between the split rings. Hence

$$\mu_{\text{eff}} = 1 - \frac{\frac{\pi r^2}{a^2}}{1 + \frac{2\sigma i}{\omega r \mu_0} - \frac{3 d c_0^2}{\pi^2 \omega^2 r^3}} \quad (2.20)$$

Since a capacitance is introduced into the system, effective permeability of the SRR becomes resonant. Figure 2.4 illustrates the generic form of  $\mu_{eff}$  for SRRs.

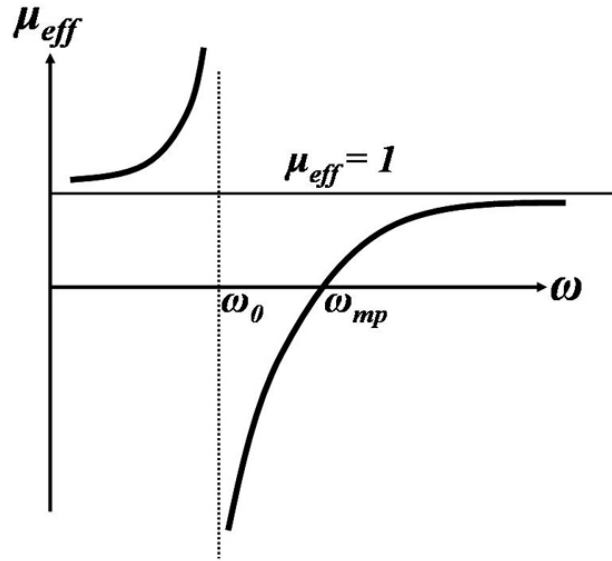


Figure 2.4: Resonance for effective permeability of SRRs [5].

$\omega_0$  is defined to be the frequency at which  $\mu_{eff}$  diverges as follows:

$$\omega_0 = \sqrt{\frac{3}{\pi^2 \mu_0 C r^3}} = \sqrt{\frac{3 d c_0^2}{\pi^2 r^3}} \quad (2.21)$$

and  $\omega_{mp}$  to be the magnetic plasma frequency

$$\omega_{mp} = \sqrt{\frac{3}{\pi^2 \mu_0 C r^3 (1-F)}} = \sqrt{\frac{3 d c_0^2}{\pi^2 r^3 (1 - \frac{\pi r^2}{a^2})}} \quad (2.22)$$

Pendry *et al.* carried through this analysis, finding a generic function for the effective permeability



$$\mu_{\text{eff}} = 1 - \frac{F\omega^2}{\omega^2 - \omega_0^2 + i\Gamma\omega} \quad (2.20)$$

Eq. (2.20) indicates that propagating modes occur up until the frequency  $\omega_0$ , followed by a gap where no propagating modes exist, followed by propagating modes starting from the frequency  $\omega_0/\sqrt{1-F}$ . The reason for the gap in propagation is of particular significance, since effective permeability will become negative for this frequency region. Turning back to Fig. 2.4, the real part of the permeability increases from unity at  $\omega = 0$  to a large positive values near  $\omega = \omega_0$ , where it then abruptly passes to a large negative value, crossing  $\mu = 0$  at  $\omega = \omega_{mp}$ . The peak value of the permeability, infinite in the case of no loss, is constrained by the magnitude of the material loss in the SRR [32]. The width of the negative permeability region is determined by the filling factor  $F$  (Eq. 2.18). At high frequencies Eq. (2.20) implies that the permeability tends toward  $1-F$ , however, it is understood that the material will stop responding at a very high frequency, and the permeability will actually reach unity.

The polarization of the electromagnetic field with respect to the SRR structure is a key issue to achieve negative values of  $\mu_{\text{eff}}$ . There are two incident polarizations of interest: magnetic field along the split ring axes,  $H_{\parallel}$  case (Fig. 2.5.(a)) and perpendicular to the split ring axes,  $H_{\perp}$  case (Fig 2.5.(b)). In both cases, the electric field is in the plane of the rings. Measurements and analyses showed that there are stop bands for both polarization cases where EM waves cannot propagate inside the medium [6]. A photonic band gap of the SRR medium does not necessarily imply that  $\mu_{\text{eff}}$  is negative. Therefore one has to check whether the gap is due to negative  $\mu_{\text{eff}}$  or negative  $\varepsilon_{\text{eff}}$  of the structures.

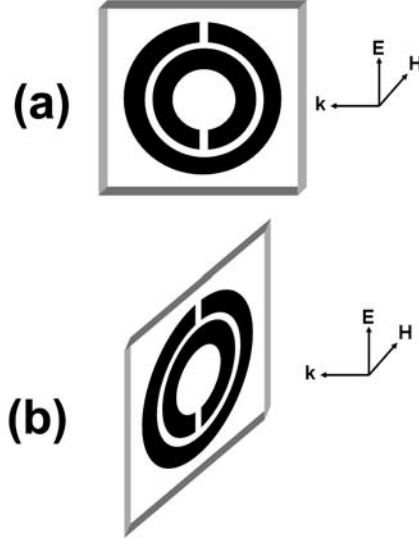


Figure 2.5: Magnetic field polarized (a) along the split ring axis,  $H_{\parallel}$  case, (b) perpendicular to the split ring axis,  $H_{\perp}$  case.

Smith *et al.* investigated the reason of the gap by altering the dielectric function of the medium and creating scattering properties that can distinguish whether the band gaps are due to either the  $\mu_{eff}$  or  $\epsilon_{eff}$  of SRR being negative [6,33]. It is shown that for  $H_{\parallel}$  case, SRRs respond to magnetic field and  $\mu_{eff}$  becomes negative over a certain frequency range. But for the  $H_{\perp}$  case, magnetic effects are small, and  $\mu_{eff}$  varies slowly and thus have a small and positive  $\mu_{eff}$  value [6]. Since the SRR structures in Fig. 2.5 are designed to be 1-Dimensional elements, we have anisotropic material. To obtain negative permeability for each polarization, one should use higher dimension SRR structures, to lift off the anisotropy of the 1D SRR structures. In chapter 4, we will show an alternative and easier way to determine the formation of band gaps of the SRRs.

## 2.4 Negative Refraction

Maxwell equations determine how electromagnetic waves propagate within a medium and can be solved to arrive at a wave equation of the form

$$\frac{\partial^2 E(x, t)}{\partial x^2} = \epsilon\mu \frac{\partial^2 E(x, t)}{\partial t^2} \quad (2.21)$$

In Eq. 2.21  $\epsilon$  and  $\mu$  enter as a product, so it is not a problem whether both their signs are positive or negative. Indeed solutions have the form of  $\exp[i(nkd - \omega t)]$ , where  $n = \sqrt{\epsilon\mu}$  is the refractive index. Propagating solutions exist in the material for two distinct cases: i)  $\epsilon > 0$  and  $\mu > 0$ , ii)  $\epsilon < 0$  and  $\mu < 0$ . So, what is the difference between positive and negative refractive indices, and why do we choose  $n$  to be negative?

Let us consider the refraction phenomena occurring when an incident beam transits from one medium into another. Suppose that the initial has a positive refractive index, therefore  $\epsilon_1 > 0$  and  $\mu_1 > 0$ . If  $\epsilon_2 > 0$  and  $\mu_2 > 0$ , we shall have an ordinary refraction case. But for the case where  $\epsilon_2 < 0$  and  $\mu_2 < 0$ , we have a beam transition from an ordinary medium into a medium with negative  $\epsilon$  and  $\mu$ . However, in every case the boundary conditions should be reached. Remember that boundary conditions require tangential components of  $\mathbf{E}$  and  $\mathbf{H}$ , and normal components of  $\mathbf{D}$  and  $\mathbf{B}$  to be continuous at the interface.

$$E_{t_1} = E_{t_2} \quad , \quad H_{t_1} = H_{t_2} \quad (2.22)$$

$$\epsilon_1 E_{n_1} = \epsilon_2 E_{n_2} \quad , \quad \mu_1 H_{n_1} = \mu_2 H_{n_2} \quad (2.23)$$

It is evident from Eqs. (2.22) and (2.23) that  $x$  and  $y$  components of the field are not changed at transition from medium 1 to 2, regardless of the signs of  $\varepsilon$  and  $\mu$ . As for the normal  $z$  components of the field, they preserve their directions if  $\varepsilon$  and  $\mu$  preserve their signs in both media; they change their directions if two media have different signs of  $\varepsilon$  and  $\mu$  [1].

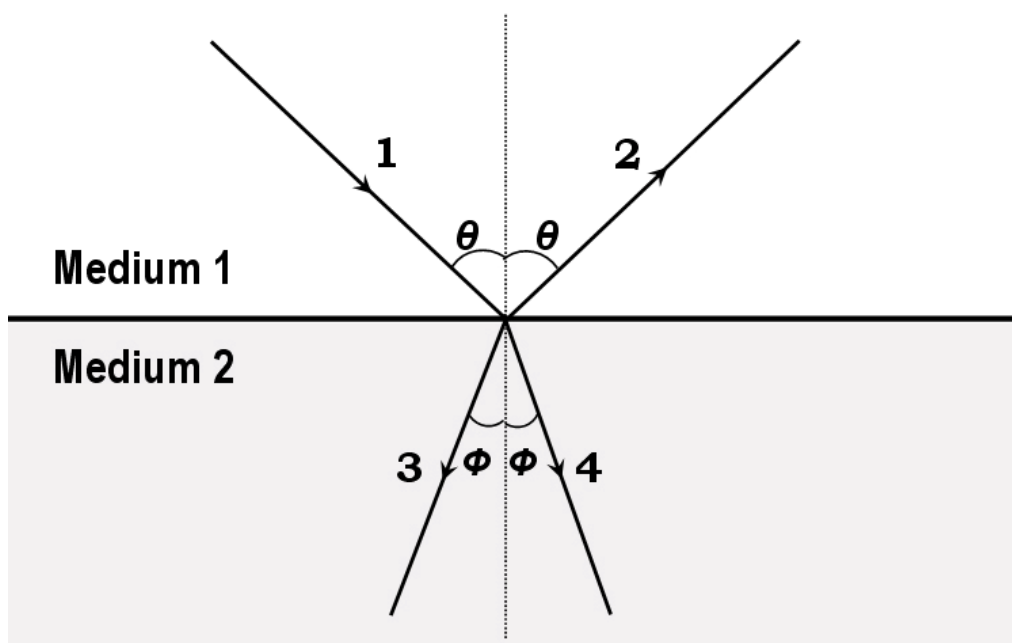


Figure 2.6: Schematic drawing of incident (1), reflected (2), negatively refracted (3) and positively refracted (4) beams.

If we consider relations (Eq. 2.6) with due reference to Eq. (2.22) and (2.23), it is immediately understood that a beam transition from a medium with positive  $\varepsilon$  and  $\mu$  into a medium  $\varepsilon < 0$  and  $\mu < 0$ , the sign of  $z$  component of  $k$  ( $k_z$ ) is reversed. The sign reversal of  $k_z$  vector corresponds to a mirror reflection of a triad,  $\mathbf{E}$ ,  $\mathbf{H}$  and  $\mathbf{k}$  in the boundary plane of two media. This means that if a

beam goes from an ordinary medium into one with negative  $\varepsilon$  and  $\mu$ , it is symmetrical compared to the case with positive  $\varepsilon$  and  $\mu$ . In other words an incident beam is refracted at the other side of the normal, which is different than the case in an ordinary refraction. Figure 2.6 sketches the path of the beams when beam 1 is transiting from medium 1 to 2. There are four beam paths as seen in the figure: 1-incident beam, 2-reflected beam, 3-refracted beam when  $n_2 < 0$ , 4- refracted beam when  $n_2 > 0$ . If the beam is assumed to be incident to medium 1 at angle  $\theta$ , the refraction angle  $\Phi$  will be negative when  $\varepsilon_2$  and  $\mu_2$  are both negative. Refractive index,  $n$ , determined by using Snell's law

$$n_1 \sin \theta = n_2 \sin \Phi \quad (2.24)$$

is also negative.

One needs to be careful when taking the square root of Eq. 2.3, because  $\varepsilon$  and  $\mu$  are analytic functions whose values are generally complex. The ambiguity in the sign of the square root can be resolved with a proper analysis of the problem. Consider that we have a material having  $\varepsilon = \mu = -1$ .  $\varepsilon$  and  $\mu$  can be written in another form as  $\varepsilon = \exp(i\pi)$  and  $\mu = \exp(i\pi)$ , then  $n = \sqrt{\varepsilon\mu} = \exp(i\pi/2)\exp(i\pi/2) = \exp(i\pi) = -1$ . The important step is that the square root of either  $\varepsilon$  or  $\mu$  alone must have a positive imaginary part, which is a necessity for passive material [34].

The  $n < 0$  solution consists of plane waves propagating toward the source, rather than plane waves propagating away from the source. Since such a solution would normally be rejected on the grounds of causality, a general

method is employed by Smith *et al* [8]. The work done by the source on the fields is given[8] as

$$P = \Omega W = -\frac{1}{2} \int_V j^* E(x, \Omega) dx = \pi \frac{\mu}{cn} j_0^2 \quad (2.25)$$

We require that the average work ( $W$ ) done by source on the fields is positive. In a right-handed medium, both  $\mu$  and  $n$  are positive, therefore  $n > 0$  solution is selected. On the other hand, in a left-handed medium since  $\mu < 0$ , we conclude that the solution with  $n < 0$  leads to the correct interpretation that the current performs positive work on the fields [8]. Since the work done by the source on the fields is positive, energy propagates outward from the source, in agreement with Veselago's proposals [1].

Negative refractive materials are necessarily frequency dispersive, so that the various frequency components of a modulated beam are refracted at different angles within the medium. Through an analysis of the points of the constant phase of a modulated plane wave, it is shown that both the group and phase velocities undergo negative refraction at the interface between a positive and a negative index material [35]. The interference fronts of the modulated wave are not normal to the group velocity, and exhibit a sideways motion as they move at the group velocity. Consideration of a modulated beam of finite extent clearly resolves the difference between the group velocity and normal to the interference fronts.

Existence of a negative refractive index implies an entirely new form of geometrical optics. A striking example is shown in Fig. 2.7(a), where a slab of

negative index material focuses the point source, which is not the case in the positive index materials. A rectangular lens made of positive index material will expectedly diverge the beam. But it is possible to focus EM waves using rectangular slab lenses made of left-handed materials. As seen in Fig. 2.7(a), EM waves cross inside the LHM slab lens (if the slab is thick enough), which implies a second focusing point, a different behavior from that of focusing in positive refractive materials. Fig. 2.7(b) shows the case when a convex lens of left-handed material is used. Different from the case in right-handed materials, waves diverge instead of converging. Fig. 2.7(c) is the case when a concave lens is used. Instead of a diverging beam, a converging beam is obtained.

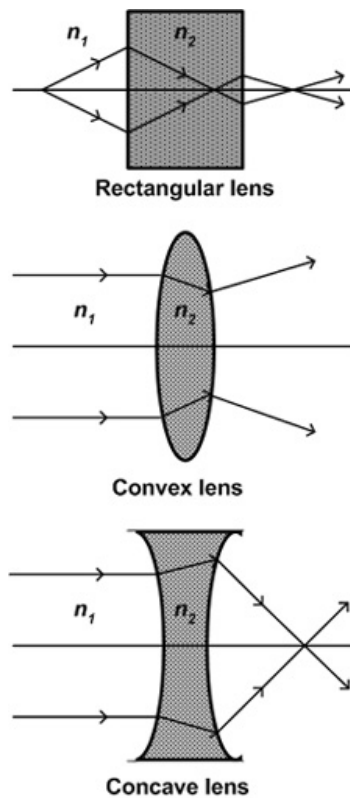


Fig 2.7: Beam path in (a) rectangular, (b) convex, (c) concave lenses made of left-handed materials.

If the permittivity and permeability and therefore refractive index is equal to -1, and the point source is close enough to the slab of a left-handed medium, impedance will be matched and therefore no reflection will occur. A slab can be designed to focus not only propagating waves, but also evanescent waves using left-handed materials. Such lenses are called “perfect lenses” [22]. Light can be brought to perfect focusing without the usual constraints imposed by the wavelength. Negative refractive index materials restore not only the phase of propagating waves, but also the amplitude of evanescent states.